Parametric Study of Eccentrically Loaded Concrete Encased Steel Composite Columns Using Artificial Neural Networks

Samoel Mahdi Saleh
Department of Civil Engineering, College of Engineering, University of Basrah
eng.samoel@gmail.com

Abstract

This paper presents a parametric study to investigate the behavior of eccentrically loaded concrete encased steel composite columns (SRC). The artificial neural network (ANN) technique was adopted in this study by developing an efficient model to predict the behavior of such composite columns, depending on a total of 105 experimental tests for such composite columns with concrete rectangular section encased I-shape structural steel section and subjected to eccentric loads producing bending moment about one of the column section axes. The developed model was used to investigate the effects on the structural behavior of the eccentrically loaded composite columns owing to the steel contribution ratio, the axis of the applied bending, the concrete strength, and the structural steel yield stress by analyzing of 36 SRC specimens with different structural properties. Generally, it is shown that the effect of the axis of applied bending moment on the strength of SRC specimens is directly proportional to steel contribution ratio. It was observed, also, that in spite of the strength of the analyzed composite columns were increased with the increase in the strength of concrete, but the both effects, the axis of the applied bending moment and the increase of structural steel yield stress, are inversely proportional to the increase of concrete strength. The Predicted strengths of SRC specimens from ANN analysis were compared with that calculated using the EC4, giving good agreement reached to a ratio around 0.96.

Keywords: Eccentrically loaded Composite Columns, Artificial Neural Network, Eurocode 4, Concrete Encased Steel Sections

الخلاصة

تم في هذا البحث دراسة لسلوك الاعمدة المغلفة كليا والمركبة من الخرسانة والحديد (SRC) تحت تأثير تحميل لامركزي. تم استخدام تقنية الشبكات العصبية الاصطناعية (ANN) في هذه الدراسة من خلال تطوير نموذج فعال للتنبؤ بسلوك هذه الأعمدة المركبة، بألاعتماد على مجموعه من الاختبارات التجريبية السابقة لمثل هذه الأعمدة المركبة وذات مقاطع مستطيلة تحتوي على مقاطع حديد ذات الشكل (I) والتي بلغ عددها 105 عينة. تم استخدام النموذج المطور من الشبكات العصبية الاصطناعية في تحليل ما يقارب 36 عينة ذات مواصفات انشائية مختلفة لتحديد مدى تأثير كل من نسبة مساهمة الحديد، محور الانحناء الاعظم ام الاصغر، مقاومة الخرسانة ، واجهاد الخضوع لمقطع الحديد على تصرف مثل هكذا اعمدة. وجد أن تأثير محور الانحناء على مقاومة الاعمدة اللتي تم تحليلها يتناسب طرديا مع نسبة مساهمة الحديد. وجد ايضا بأنه وعلى الرغم من الزيادة في مقاومة الاعمدة المغلفة كليا والمركبة من الخرسانة والحديد بزيادة مقاومة الخرسانة الا أن تأثير محور الانحناء واجهاد الخضوع لمقطع الحديد على تصرف هذه الاعمدة يتناسب عكسيا مع الزيادة في مقاومة الخرسانة. كل النتائج المستنبطة من استخدام تقنية الشبكات العصبية الاصطناعية تم مقارنتها مع تلك المحسوبة بأستخدام الطريقة المعتمدة في الكود الاوربي (EC4). حيث وجد بأن معدل نسبة المطابقة بين النتائج وصل الى (0.96).

الكلمات المفتاحية: الاعمدة المركبة من الخرسانة والحديد، تحميل لامركزي، الشبكات العصبية الاصطناعية، الكود الاوربي.

1. Introduction

The high loading bearing capacity for relatively small sections and the sections with different load bearing capacities, but identical dimensions represent some of the characteristics of the concrete encased steel composite columns that provide various advantages and then facilities to solve different problems in the design and construction of different structures. Therefore, this type of composite construction is being increasingly used in a wide range of structural applications.

Various experimental and numerical studies were investigated the structural behavior of concentrically loaded, and eccentrically loaded concrete encased steel composite columns and the others investigated the structural behavior of concrete encased steel beam-columns. One of these researches was conducted by Stavens in 1965, who tested thirty-five steel-concrete composite columns under axial compression and twenty-four steel-concrete composite columns under eccentric compression to study the effect of the slenderness ratio on the ultimate load and the effect of the combination of compression and bending on the total behavior of such composite columns. In 1978, Johnson and May tested eight encased steel-concrete composite columns elastically restrained about one or both axes in order to investigate the effect of composite columns effective length on their ultimate carrying capacities and compared the results with that calculated according to the method of BS 5400 – Part 5. Mirza et. al., at 1996, tested sixteen specimens of concrete encased steel composite beam-column to develop a wide range of applied loads with different external eccentricities taking into account the second order effects into account. They compared their test results with the analysis based on ACI 318, Eurocode 4, and finite-element modeling, also they concluded that the ultimate strength of such composite members slightly affected by bonding condition at the interface of steel rib connectors and the surrounding concrete. Weng and Yen, in 2002, compared between two approached for the design method of concrete encased steel composite columns that developed by ACI 318 code (1999) and AISC-LRFD specification (1993). This comparative study indicates that the ACI-318 approach generally gives closer predictions than the AISC-LRFD does with the experimented results that done by previous researchers. In 2011 a nonlinear 3-D finite element model for eccentrically loaded concrete encased steel composite column presented by Ellobody et al. in order to investigate the behavior of such columns taking into account the effect of different design parameters such that the compressive strength of the concrete, the yield strength of the structural steel section, and the value of the eccentricity for the applied compressive load.

As knowing, in the presence of bending moment, the resistance of the concrete encased steel composite column sections to axial compression decreases. In this case, the resistance of any such column cross sections will be enough to the applied loads when the combination of the applied axil compression and bending moment lies inside the area of the failure curve (interaction curve) that developed from the relation between the section ultimate axial resistance to compression and the ultimate resistance to bending.

By the present work, a parametric study was carried out to investigate the effects of some important parameters on the behavior of eccentrically loaded concrete encased steel composite columns (SRC). These parameters were the steel contribution ratio, the axis of applied bending (bending about major or minor axis of section), the grade of concrete, and the grade of structural steel. The artificial neural networks (ANN) technique was adopted in this study, depending on a database that collected from experimental test results provided related to previous researchers. Finally, the results evaluated by the predicted ANN were compared with the design and analysis approach provided by Eurocode 4.

2. Review of EC4 Approach

Eurocode 4 (EN 2004) adopted a simplified method for analysis and design of steel-concrete composite columns having doubly symmetrical and uniform cross section. Under uniaxial compression, the compressive strength, N_{pl}, of a concrete encased steel composite column can be evaluated by summing up the axial load capacities of the materials that make up the cross section. This leads to;

$$N_{pl} = A_s \cdot f_{ys} + 0.85\, A_c \cdot f_c + A_r \cdot f_{yr} \qquad (1)$$

Where:

- A_s, A_c and A_r are the cross-sectional area of structural steel shape, concrete and reinforcement, respectively.
- f_{ys}, f_c and f_{yr} are the nominal value of the yield stress of structural steel, the characteristic value of the 150 × 300 mm cylinder compressive strength of concrete at 28 days and the nominal value of the yield stress of reinforcing steel, respectively.

On the other hand, Eurocode 4 predicted a ratio which called the relative slenderness in order to evaluate instability effects due to compression on the strength of such composite columns. The relative slenderness (λ) for the plane of bending being considered is given by;

$$\lambda = \sqrt{\frac{N_{pl}}{N_{cr}}} \qquad (2)$$

Where:

- N_{cr} is the elastic critical normal force and is given as;

$$N_{cr} = \frac{\pi^2 (EI)_{eff}}{L^2} \qquad (3)$$

- $(EI)_{eff}$ is the effective flexural stiffness and is given by;

$$(EI)_{eff} = E_s I_s + 0.6 E_{cm} I_c + E_r I_r \qquad (4)$$

- I_s, I_c and I_r are the second moment of area of the structural steel section, the un-cracked concrete section and the steel reinforcement, respectively.
- E_s, E_r, and E_{cm} are the modulus of elasticity for structural steel, reinforced steel and the secant modulus of elasticity for concrete.

If the second order effects were not considered, then the Eurocode 4 unfactored eccentric load strength was based on the cross-section and column axial force-bending moment strength interaction diagrams. For SRC subjected to bending about their major axis, the axial force- bending moment interaction diagram can be approximated by four points polygon. On the other hand, the axial force- bending moment interaction diagram for SRC that subjected to bending about their minor axis can be approximated by five points polygon. Therefore, the ultimate eccentric load of an SRC is represented by a point on the axial force- bending moment interaction diagram, and must be less the evaluated resistance of SRC under pure axial compression, N_{Rd} from the equation below.

$$N_{Rd} = \varkappa\, N_{pl} \qquad (5)$$

Where:

$$\varkappa = \frac{1}{\phi^2 + \sqrt{\phi^2 - \lambda^2}} \qquad (6)$$

$$\phi = 0.5(1 + \alpha(\lambda - 0.2) + \lambda^2) \qquad (7)$$

- χ is the reduction factor for the relevant buckling mode.
- α is the imperfection factor and is equal to 0.34 for buckling about section major axis and 0.49 for buckling about section minor axis.

3. Description of the Simulated Database

The main step in the present work is to develop an artificial neural network (ANN) model, depending on a simulated database, to predict the behavior of concrete encased steel composite columns (SRC), in order to use it in the analysis that required for the parametric study for the behavior of SRC.

A total of 105 experimental tests were compiled for the eccentrically loaded concrete encased steel composite columns (SRC), with rectangular cross sections and having I-shape steel section. These experimental results were distributed on five previous studies for different researchers, as shown in table (1). In 61 of these tests, the SRC were subjected to eccentric loads producing bending moment about their major axis, whereas the remaining 44 tested SRC specimens were subjected to eccentric loads producing bending moment about their minor axis.

Table (2) below summarizes the main characteristics and the range of values for the experimentally tested SRC in the collected database that used in the present study to develop the required artificial neural network.

Table (1): Summary for Experimental Tests Database

Reference	**Numbers of Tested Specimen**
Stevens, 1965	24
Yokoo *et.al.,* (as cited in (Weng and Yen, 2002))	19
Loke, 1968	13
Roik *et.al.,* (as cited in (Kim, 2005))	34
Han and Kim, 1995	15

Table (2): Description and Ranges of Experimental Tests Database

Variable	**Minimum**	**Maximum Value**
Compressive Strength of Concrete (MPa)	11.5	46.8
Yield Stress of Structural Steel (MPa)	223	400
Yield Stress of Reinf. Steel (MPa)	276	635
Section Dimensions, B×D, (mm)	160 × 160	300 × 400
Area of Steel Section (mm^2)	970	13100
Area of Steel Reinforcement (mm^2)	0	2470
Column effective Length, kL (mm)	630	8000
Eccentricity for Bending about Major Axis (mm)	20	370
Eccentricity for Bending about Minor Axis (mm)	10	210

4. Artificial Neural Network Modeling

Artificial neural network (ANN) represents an intelligent technique to build models of networks that simulate the working of the neural network in the human brain. ANN represents an arrangement of collections of simple processing units called neurons (also called as “nodes”). These neurons represent the basic units of any ANN and by which the network is able to solve any problem by learning from previous experience (Yousif and Abdulla, 2009).

There are three main different structures to develop an ANN, depending on the data transformation in that network, which are feed-forward neural networks, feedback neural networks, and auto associative neural networks. But all of these structures have the same arrangement, where, neurons are arranged in three different layers and connected together. In the present work, the feed-forward multilayer neural network was adopted.

Three kinds of layers are used in the adopted feed-forward multilayer network model, input layer, output layer, and two hidden layers. The input layer has nine neurons as the number of parameters that considered to describe each one of SRC in the database that defined in table (2), whereas the output layer has only one neuron representing the ultimate load of SRC as output. There is no specific rule in order to determine the number of hidden layers and their neurons. Here, the number of neurons in the two hidden layers was selected after several trail networks to get best results. The first hidden layer is chosen to have nine neurons, whereas the second hidden layer is chosen to have seven neurons. The pattern of the adopted neural network is shown in figure (1).

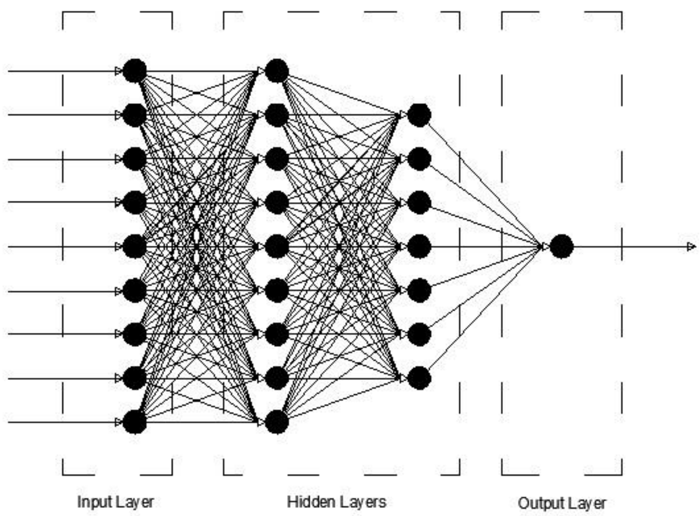

Figure (1): Artificial Neural Network Pattern

In the adopted feed-forward multilayer neural network model showing in figure (1), the data transfer with processing from the input layer to the output layer to get results thought the hidden layers. As shown in the figure, each neuron in the input layer is connected with all neurons in the first hidden layers and each neuron in the first hidden layer is also connected to all neurons in the second hidden layer, and finally all the neuros in the second hidden layer is sharing to get the output neuron its value. Each connection between two neurons has numerical strength called weight, therefore each neuron has an activation value resulting from the received inputs through the weighted connections from the other neurons.

The process through which the adopted ANN model to be able to provide an accurate output for the required study is known as training. The network training is started with a set of training data with known outputs called targets. The second step is the use of randomly selected weights for the connections to get the output. Then, the output is compared with targets for all training data. Subsequently the weights are adjusted to reach the best ANN with best connection weights to get best results. BFGS

Quasi-Newton algorithm is used for training the adopted neural network in this study. The previously described database was presented to the adopted ANN model for the training process. The total database was divided into two parts, 90% of it, which was selected randomly, was used for training the ANN model and the remaining 10% was used to test it to verify its ability to prediction.

The performance function that adopted in the current study is the mean square error (MSE). This function is represented as a criterion for the ANN during the training to reach to the best output prediction. The mean square error can be calculated as shown in equation (8) below, where, n is the total number of the data, t is the target value, and y is the output value.

$$MSE = \frac{1}{n}\sum_{1=1}^{n}(t_i - y_i)^2 \tag{8}$$

After several training times for the adopted ANN, the model with highest performance has chosen. The performance is evaluated by a regression analysis with a regression coefficient R. The regression coefficient that achieved by comparing the experimental values of the ultimate load for the data SRC (targets) with the values that predicted by ANN (output) was (0.99878) for the training 90% of the data and was (0.96834) for the testing 10% of the data. Figure (2) shows the relations between the actual ultimate loads to the corresponding ANN predicted values for training and testing data of eccentrically loaded concrete encased steel composite columns.

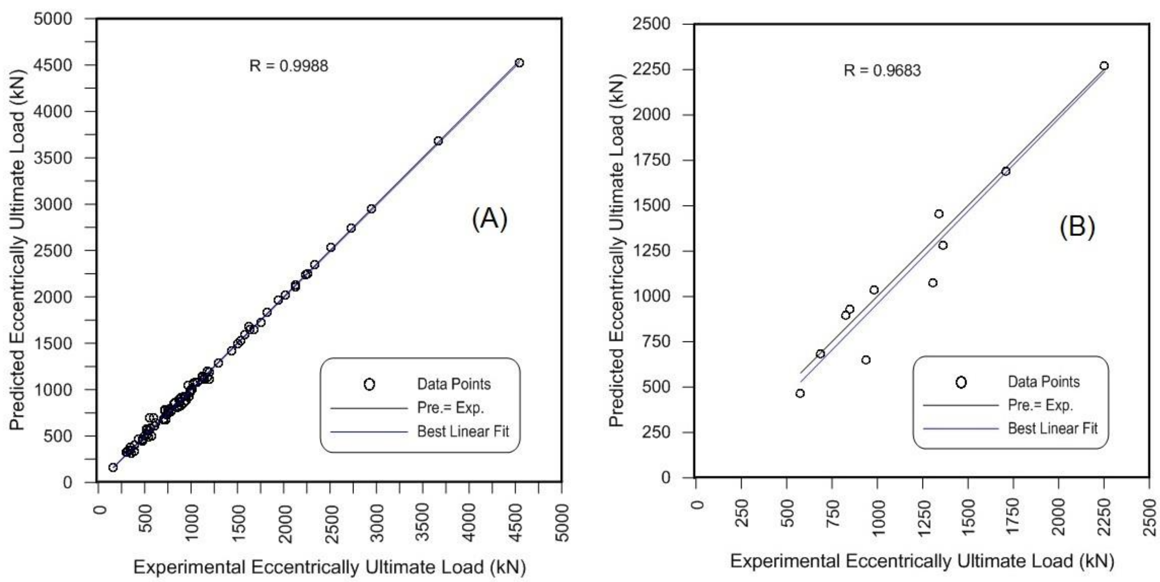

Figure (2): Scatter Diagram for Experimental to Predicted SRC Eccentrically Ultimate Load with Best Linear Fit (A: for training data, B: for testing data)

5. Parametric Study and Discussion

The verified artificial neural network (ANN) model was used in conducting an extensive parametric study. A total of 36 eccentrically loaded concrete encased steel composite columns where analyzed by ANN that having different section properties and materials. Figure (3) and table (3) summarize all the column details of the analyzed SRC in this study, which were divided into eight groups depending on the main parameter that required to study its effect on the behavior of these columns. The parameters that carried out in the study were the steel contribution ratio, the axis of applied bending (bending about major or minor axis of column section), the grade of concrete, and the grade of structural steel.

As detailed in table (3), the main parameter that considered in the first four groups of the analyzed SRC specimens (G1 to G4) was the steel contribution ratio that represented by the change of the steel section with fixing the dimensions of the overall columns section. The effect of steel contribution ratio was considered in conjunction with other effects. The concrete grade in the first two groups (G1 and G2) was taken as 25 MPa, whereas in the second two groups (G3 and G4) was taken as 35 MPa. In the same time, the axis of applied bending was the section major axis for the two groups (G1 and G3), but was the minor axis for the two groups (G2 and G4). On the other hand, the main parameter that considered in the remaining four groups (G5 to G8) was the variation of the grade of concrete, which is also considered in conjunction with other effects. The grade of the structural steel was taken equal to 275 MPa for the two groups (G5 and G6), whereas in the two groups (G7 and G8) was 355 MPa. Also, the axis of applied bending for the two groups (G5 and G7) was the major axis, but was the minor axis for the two groups (G6 and G8). It must be noted that the steel contribution ratio (δ) was evaluated according to EC4 by the following equation;

$$\delta = \frac{A_S \cdot f_{ys}}{A_S \cdot f_{ys} + 0.85\, A_C \cdot f_C + A_r \cdot f_{yr}} \tag{9}$$

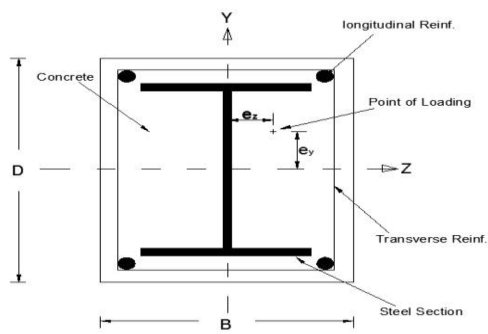

Figure (3): Typical Cross Section for Analyzed Eccentrically Loaded SRC

Table (3): Specimen Dimensions and Material Properties of Eccentrically Loaded SRC in The Parametric Study

Group	Specimen	Section, B × D (mm)	Length, kL (mm)	Steel Section	Longitudinal Steel Reinforcement	e_y (mm)	e_z (mm)	Concrete, f_c (MPa)	Steel Section. f_{ys} (MPa)	Steel Reinf0rcemet, f_{yr} (MPa)
G1	S01	300 × 300	2500	HE140A	4 ϕ 12mm	50	0	25	275	410
	S02	300 × 300	2500	HE160B	4 ϕ 12mm	50	0	25	275	410
	S03	300 × 300	2500	HE200B	4 ϕ 12mm	50	0	25	275	410
	S04	300 × 300	2500	HE180M	4 ϕ 12mm	50	0	25	275	410

Table (3): Continued

Group	Specimen	Section, B × D (mm)	Length, kL (mm)	Steel Section	Longitudinal Steel Reinforcement	e_y (mm)	e_z (mm)	Concrete, f_c (MPa)	Steel	
									Section. f_{ys} (MPa)	Reinf0rcemet, f_{yr} (MPa)
G2	S05	300 × 300	2500	HE140A	4 ϕ 12mm	0	50	25	275	410
	S06	300 × 300	2500	HE160B	4 ϕ 12mm	0	50	25	275	410
	S07	300 × 300	2500	HE200B	4 ϕ 12mm	0	50	25	275	410
	S08	300 × 300	2500	HE180M	4 ϕ 12mm	0	50	25	275	410
G3	S9	300 × 300	2500	HE140A	4 ϕ 12mm	50	0	35	275	410
	S10	300 × 300	2500	HE160B	4 ϕ 12mm	50	0	35	275	410
	S11	300 × 300	2500	HE200B	4 ϕ 12mm	50	0	35	275	410
	S12	300 × 300	2500	HE180M	4 ϕ 12mm	50	0	35	275	410
G4	S13	300 × 300	2500	HE140A	4 ϕ 12mm	0	50	35	275	410
	S14	300 × 300	2500	HE160B	4 ϕ 12mm	0	50	35	275	410
	S15	300 × 300	2500	HE200B	4 ϕ 12mm	0	50	35	275	410
	S16	300 × 300	2500	HE180M	4 ϕ 12mm	0	50	35	275	410
G5	S17	300 × 300	2500	HE200B	4 ϕ 12mm	50	0	20	275	410
	S18	300 × 300	2500	HE200B	4 ϕ 12mm	50	0	25	275	410
	S19	300 × 300	2500	HE200B	4 ϕ 12mm	50	0	30	275	410
	S20	300 × 300	2500	HE200B	4 ϕ 12mm	50	0	35	275	410
	S21	300 × 300	2500	HE200B	4 ϕ 12mm	50	0	40	275	410
G6	S22	300 × 300	2500	HE200B	4 ϕ 12mm	0	50	20	275	410
	S23	300 × 300	2500	HE200B	4 ϕ 12mm	0	50	25	275	410
	S24	300 × 300	2500	HE200B	4 ϕ 12mm	0	50	30	275	410
	S25	300 × 300	2500	HE200B	4 ϕ 12mm	0	50	35	275	410
	S26	300 × 300	2500	HE200B	4 ϕ 12mm	0	50	40	275	410
G7	S27	300 × 300	2500	HE200B	4 ϕ 12mm	50	0	20	355	410
	S28	300 × 300	2500	HE200B	4 ϕ 12mm	50	0	25	355	410
	S29	300 × 300	2500	HE200B	4 ϕ 12mm	50	0	30	355	410
	S30	300 × 300	2500	HE200B	4 ϕ 12mm	50	0	35	355	410
	S31	300 × 300	2500	HE200B	4 ϕ 12mm	50	0	40	355	410
G8	S32	300 × 300	2500	HE200B	4 ϕ 12mm	0	50	20	355	410
	S33	300 × 300	2500	HE200B	4 ϕ 12mm	0	50	25	355	410
	S34	300 × 300	2500	HE200B	4 ϕ 12mm	0	50	30	355	410
	S35	300 × 300	2500	HE200B	4 ϕ 12mm	0	50	35	355	410
	S36	300 × 300	2500	HE200B	4 ϕ 12mm	0	50	40	355	410

The predicted ultimate eccentric loads for the analyzed specimen groups (G1 to G4) are shown in table (4) for the both ANN and EC4 approaches of analysis. The variations of the ANN predicted values of eccentrically loaded SRC strength with the steel contribution ratio of the analyzed first four groups of specimens are shown in figure (4).

Table (4): ANN and EC4 Predictions for Eccentrically Loaded SRC for Tested Groups (G1 to G4)

Group	Specimen	Steel Contribution Ratio	ANN		EC4		P_{ANN} / P_{EC4}
			P_{ANN}	M_{ANN}	P_{EC4}	M_{EC4}	
G1	S01	0.29	1792	89.6	1898	94.9	0.94
	S02	0.42	2412	120.6	2219	111.0	1.09
	S03	0.52	2787	139.4	2680	134.0	1.04
	S04	0.62	3084	154.2	3197	159.8	0.96
G2	S05	0.29	1670	83.5	1887	94.4	0.88
	S06	0.42	2097	104.9	2160	108.0	0.97
	S07	0.52	2381	119.1	2477	123.8	0.96
	S08	0.62	2573	128.7	2852	142.6	0.90
G3	S09	0.23	2009	100.5	2377	118.8	0.85
	S10	0.35	2716	135.8	2733	136.6	0.99
	S11	0.44	3167	158.4	3171	158.6	0.99
	S12	0.55	3591	179.5	3664	183.2	0.98
G4	S13	0.23	1874	93.7	2312	115.6	0.81
	S14	0.35	2427	121.4	2677	133.9	0.91
	S15	0.44	2795	139.8	2993	149.7	0.93
	S16	0.55	3132	156.6	3362	168.1	0.93
Mean	---	---	---	---	---	---	0.95

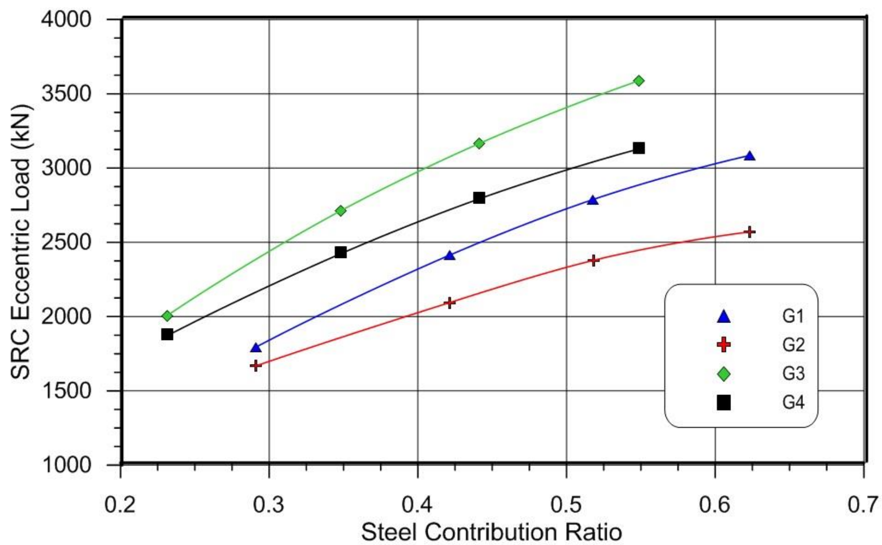

Figure (4): SRC Eccentric Load – Steel Contribution Ratio Relationships

It is clearly shown in table (4) and figure (4) that the ultimate eccentric load for the analyzed SRC specimens is increased with the increase of the steel contribution ratio whether the applied bending was about the major or minor axis of SRC section. Also, it can be seen in figure (4) that by fixing the overall dimensions of SRC section and increasing the steel contribution ratio, the effect of axis of bending is increased on the SRC ultimate eccentric load with the increase of steel contribution ratio. This is related to the role of the concrete, in the case of low steel contribution ratio, to resist the applied bending of such type of composite columns. On the other hand, with the increase of concrete strength from 25MPa to 35MPa for the analyzed SRC specimens with applied bending about the major axis, the steel contribution ratio was decreased with an average value about 24%, but the ultimate eccentric compressive load was increased with a ratio ranged from about 12% for (S01/S09) specimens that having the lower steel contribution ratio to about 16% for (S04/S12) specimens that having the upper steel contribution ratio. This response can be seen also for specimens that analyzed with applied bending about minor axis.

Table (5) presented the predicted ANN and EC4 ultimate eccentric loads for the analyzed specimen of the groups (G5 to G8). The predicted ANN ultimate eccentric loads were plotted against the concrete strength for the four groups, as shown in figure (5).

Table (5): ANN and EC4 Predictions for Eccentrically Loaded SRC for Tested Groups (G5 to G8)

Group	**Specimen**	**Steel Contribution Ratio**	**ANN**		**EC4**		**P_{ANN} / P_{EC4}**
			P_{ANN}	**M_{ANN}**	**P_{EC4}**	**M_{EC4}**	
G5	S17	20	2749	137.5	2435	121.7	1.13
	S18	25	2890	144.5	2680	134.0	1.08
	S19	30	3037	151.9	2925	146.3	1.04
	S20	35	3208	160.4	3171	158.6	1.01
	S21	40	3427	171.3	3418	170.9	1.00
G6	S22	20	2130	106.5	2216	110.8	0.96
	S23	25	2280	114.0	2477	123.8	0.92
	S24	30	2493	124.7	2735	136.8	0.91
	S25	35	2724	136.2	2993	149.7	0.91
	S26	40	3012	150.6	3250	162.5	0.93
G7	S27	20	3097	154.9	2817	140.9	1.10
	S28	25	3177	158.9	3063	153.2	1.04
	S29	30	3286	164.3	3309	165.4	0.99
	S30	35	3453	172.7	3554	177.7	0.97
	S31	40	3630	181.5	3799	189.9	0.96
G8	S32	20	2375	118.7	2492	124.6	0.95
	S33	25	2530	126.5	2757	137.9	0.92
	S34	30	2694	134.7	3020	151.0	0.89
	S35	35	2871	143.6	3281	164.0	0.88
	S36	40	3107	155.4	3540	177.0	0.88
Mean	---	---	---	---	---	---	0.97

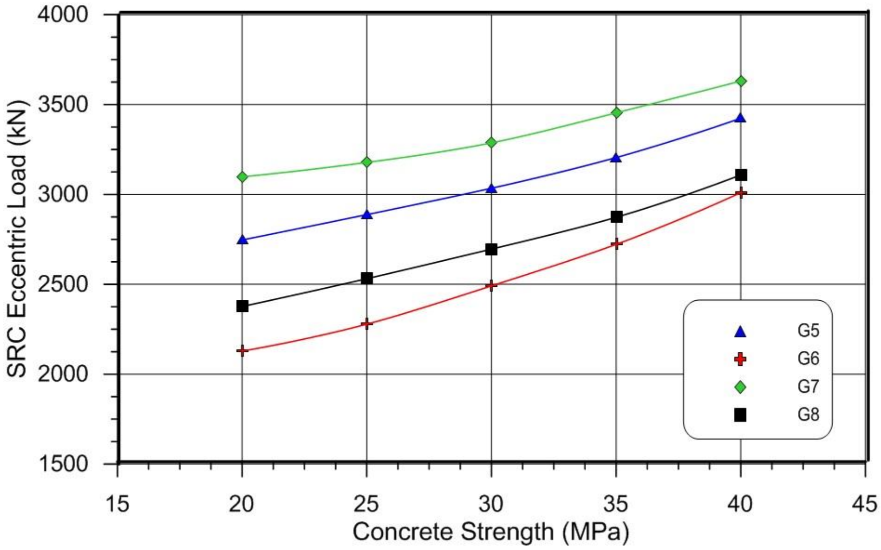

Figure (5): SRC Eccentric Load – Concrete Strength Relationships

It is clearly shown in figure (5) that with the increase of the concrete strength, the ultimate eccentric load of analyzing SRC specimens was increased. But unlike that observed in the relation of eccentric load with steel contribution ratio, the effect of axis of bending (major or minor) decreases with the increase of the concrete strength of SRC section. This is appeared numerically in table (5), if compared the predicted values of the analyzed specimens of the two groups G5 and G6, where the corresponding relationships of these two groups between eccentric load and concrete strength and as shown in the figure (5) is started with a difference between them of about 619 kN (corresponding to 20 MPa of concrete strength), whereas they are ended with a difference of about 415 kN (corresponding to 40 MPa of concrete strength) taking into account that the analyzed specimens of G5 were bent about their major axis but the analyzed specimens of G6 were bent about their minor axis. The same response was observed according to the results that predicted for the two groups G7 and G8, where the only difference between them and G5 and G6, respectively, is the structural steel yield stress. On the other hand, it can be seen that with the increase of concrete strength the effect of the structural steel yield stress on the eccentric load is decreased for specimens that bent about the same axis, as clearly shown between G5 and G7 or between G6 and G8 in figure (5), Generally, the increase in the yield stress of steel section for analyzed SRC specimens from 275MPa (G5 and G6) to 355 MPa (G7 and G8), produced an average increase in the ultimate eccentric loads about 10% for specimens that bent about their major axis (G5 and G7) and about 8% for specimens that bent about their minor axis (G6 and G8), when the concrete strength increased from 20 to 40 MPa.

6. Comparison with EC4 Design Guides

The ultimate eccentric loads for the analyzed SRC specimens that obtained from the ANN analysis approach were compared with the unfactored design SRC eccentric loads calculated using the EC4 simplified method [6], as shown in tables (4) and (5). The eccentric SRC loads that obtained from ANN and EC4 were also plotted in figures (6) to (9). Looking at tables (4) and (5), generally, it can be seen that the range of (P_{ANN} / P_{EC4}) values were from 1.09 to 0.81 for the first four analyzed groups with a mean value of 0.95, whereas the range for the last four groups were from 1.13 to 0.88 with a mean value of 0.97. This variation in the values of the ratio of the ANN predicted eccentric loads to these calculated using EC4 may be related to that the ANN predicted values are actually completely depended on the actual behavior of experimentally tested SRC specimens. Therefore, and as shown in tables (4) and (5), the (P_{ANN} / P_{EC4}) ratios of some analyzed specimens were less than one and others were larger than one. In spite of the discrepancy between the ANN and EC4 predictions, the responses of the analyzed SRC specimens for the adopted parameters in this study are approximately same for both analysis techniques. But, and as mentioned earlier, the ANN analysis shown that the effect on the SRC strength owning to the increase of structural steel yield stress is reduced with the increase of concrete strength. This was not clearly predicted according to EC4, as shown in figures (8 and (9).

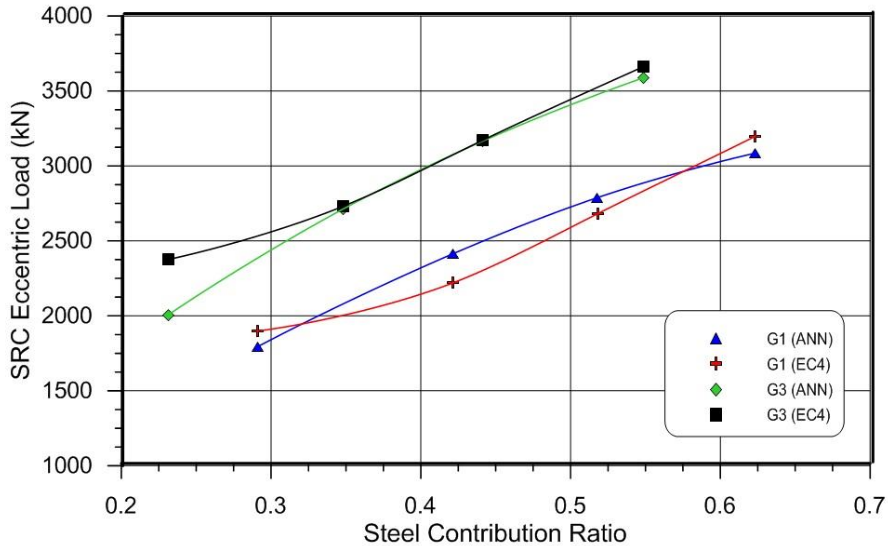

Figure (6): Comparison of ANN and EC4 Results for Groups (G1 and G3)

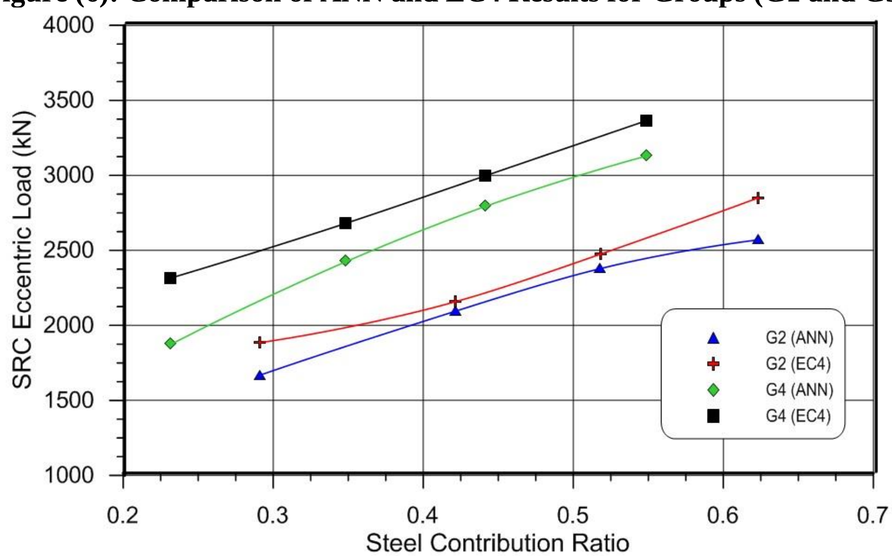

Figure (7): Comparison of ANN and EC4 Results for Groups (G2 and G4)

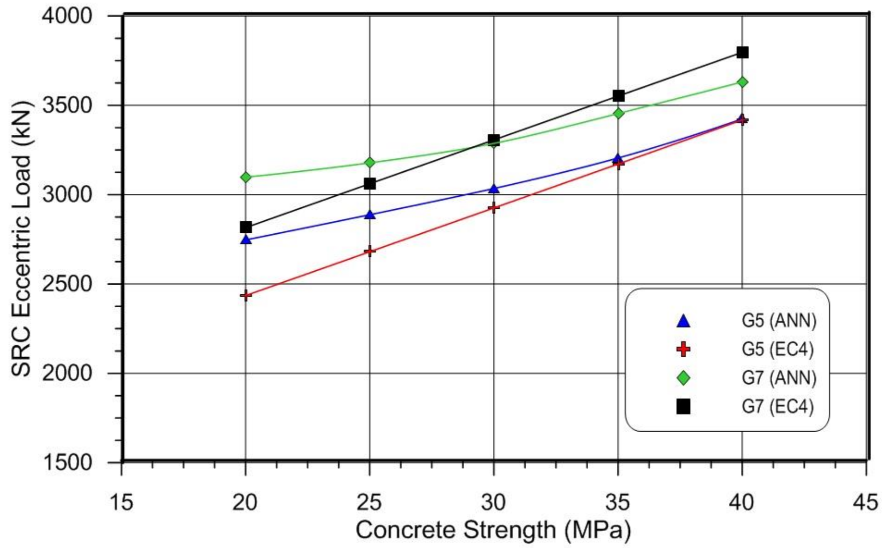

Figure (8): Comparison of ANN and EC4 Results for Groups (G5 and G7)

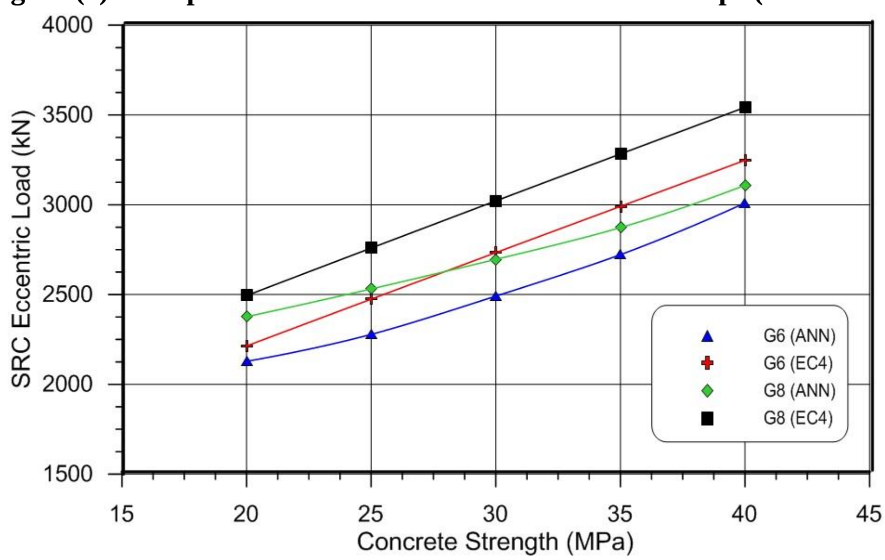

Figure (9): Comparison of ANN and EC4 Results for Groups (G6 and G8)

The axial load – bending moment interaction diagrams for SRC specimens investigated in this parametric study were plotted according to the simplified method in the EC4. Figures (10) to (13) show the interaction diagrams plotted for group (G1), group (G2), specimens S12 with S16, and specimens S23 with S33.

Figures (10) and (11) show the effect of steel contribution ratio and the concrete strength, respectively, on the strength of SRC sections that analyzed according to EC4 with bent of about major axis. it can be shown from these figures that with increase the steel contribution ratio or concrete strength, the size of overall interaction diagram was also increasing. But, at the points of maximum bending moment for the interaction diagrams in figure (10), the axial load value slightly decreases with increase the steel contribution ratio, whereas in figure (11) the axial load at the same points in significantly increased with increase the concrete strength of SRC section. This is completely related to the method of developing these interaction diagrams adopted by EC4, in which the axial load at these points completely depending on the area and strength of the concrete part of the SRC section (Schleich and Chantrain, 1998). Figure (12) clearly shows the variation in the size of interaction diagrams for the strength of SRC section, which have steel contribution ratio equal to 0.55, concrete strength of 35 MPa, and structural steel yield stress of 275 MPa, due to the change of the axis of the applied bending moment from major to minor axis. Looking at figure (13), the effect of increase the structural steel yield stress from 275 to 355 MPa, keep anything else the same, on the size of the interaction diagram of the related specimens is clearly shown.

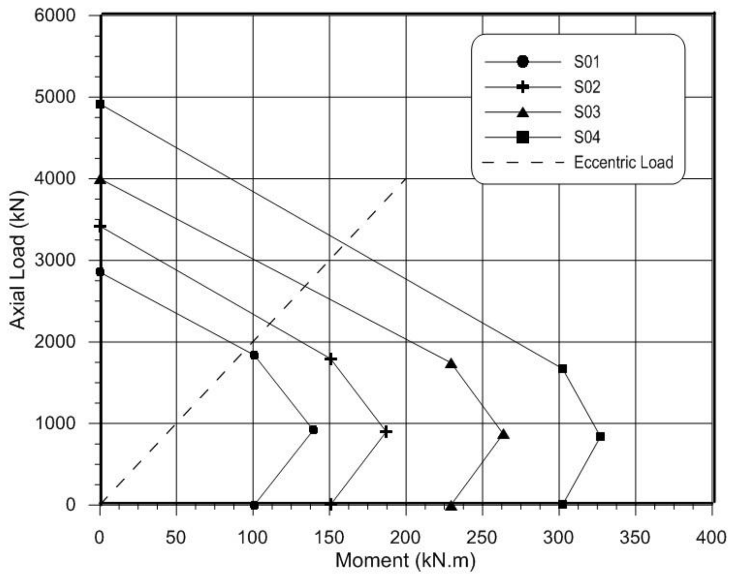

Figure (10): Interaction Diagrams for SRC Specimens of Group G1

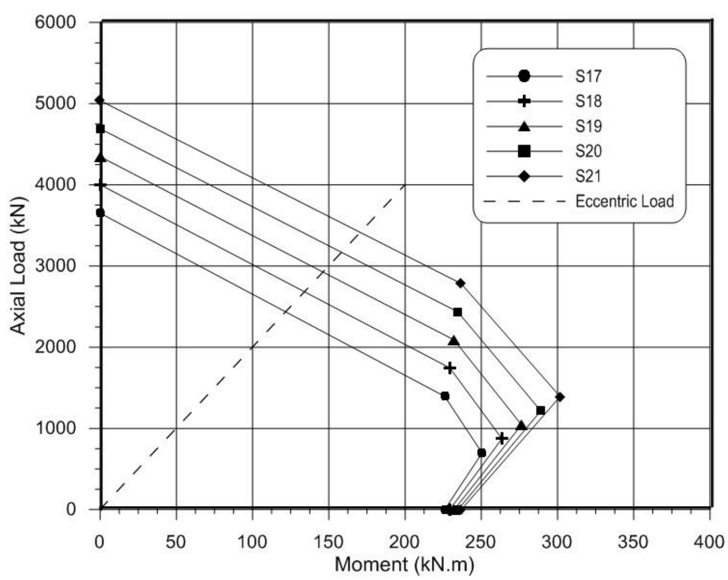

Figure (11): EC4 Interaction Diagrams for SRC Specimens of Group G5

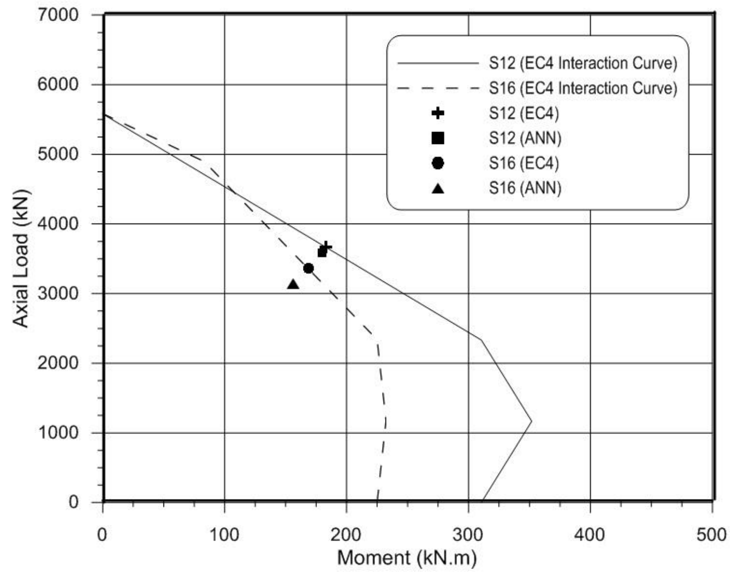

Figure (12): EC4 Interaction Diagrams for S12 and S16 SRC Specimens

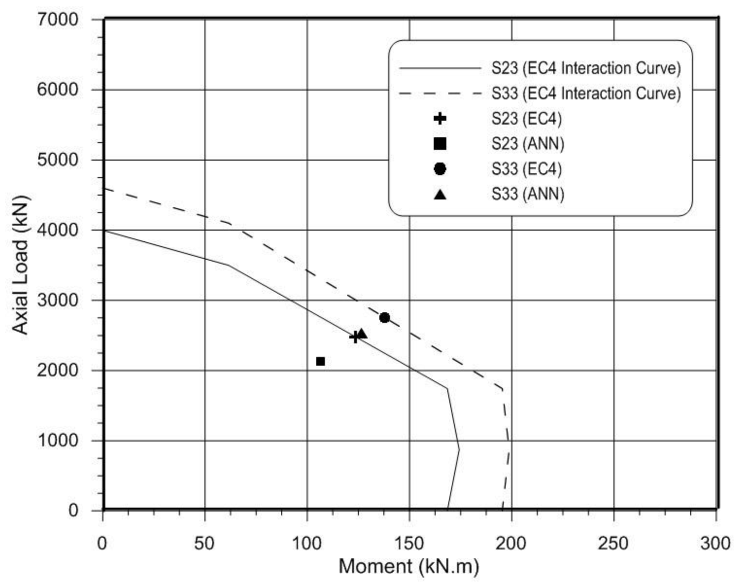

Figure (13): EC4 Interaction Diagrams for S23 and S33 SRC Specimens

7. Conclusions

A parametric study was adopted to consider the behavior of eccentrically loaded concrete encased steel composite column. An artificial neural network model has been developed for the analysis of the columns. The developed model was used to investigate the effects on the structural behavior of the eccentrically loaded composite columns owing to the steel contribution ratio, the axis of applied bending the concrete strength, and the structural steel yield stress. Generally, it is shown that the effect of the axis of applied bending moment on the strength of SRC specimens is directly proportional with steel contribution ratio. It was observed, also, that in spite of the strength of the analyzed composite columns were increased with the increase in the strength of concrete, but the both effects, the axis of applied bending moment and the increase of structural steel yield stress, are inversely proportional with the increase of concrete strength. The Predicted strengths of SRC specimens from ANN analysis were compared with that calculated using the EC4, giving good agreement reached to a ratio around 0.96.

References

Designers' guide to EN 1994, 2004, "EUROCODE 4: Design of Steel and Concrete Composite Structures", Part 2: General Rules and Rules for Bridges, CEN.

Ellobody E. Ben Y., and Dennis L., 2011, "Eccentrically loaded concrete encased steel concrete composite columns", Thin Walled Structures, Vol. 49, pp. 53-65.

Han D. J. and Kim, K. S., 1995, "A study on the Strength and Hysteretic Characteristics of Steel Reinforced Concrete Columns," Journal of the Architectural Institute of Korea, Vol. 11, No. 4, pp. 183-190.

Johnson R. P. and May I. M., 1978, "Tests on restrained composite columns", The Structural Engineer, Vol. 56, No. 2, pp. 21-28.

Kim D. K., 2005, "A database for composite columns", M.Sc. Thesis, Georgia Institute of Technology.

Loke, Y. O., 1968, "The behavior of composite steel concrete columns", Ph.D. Dissertation, University of Sydney, Sydney.

Mirza A. S., Hyttinen V., and Hyttinen E., 1996, "Physical tests and analysis of composite steel-concrete beam-columns", Journal of Structural Engineering, Vol.122, No. 11, pp. 1317-1326.

Schleich J. B. and Chantrain Ph., 1998, "Simplified version of Eurocode 4 for usual buildings", A report submitted by Technical Steel Research, European Communities, Luxembourg.

Stevens R. F., 1965, "Encased stanchions", The Structural Engineer, Vol.43, No. 2, pp. 59-66.

Weng C. C. and Yen S. I., 2002, "Comparisons of concrete-encased steel composite columns strength provisions of ACI code and AISC specifications", Engineering Structures, Vol. 24, pp. 59-72.

Yousif S. T. and Abdulla S. M., 2009, "Artificial neural network model for predicting compressive strength of concrete", Tikrit Journal of Engineering Sciences, Vol. 16, No. 3, pp. 55-66.